FULL PAPER

BJC

British Journal of Cancer (2014) 111, 1350–1362 | doi: 10.1038/bjc.2014.437

Keywords: soft tissue sarcoma; solitary fibrous tumour; anti-angiogenic therapy; anti-tumour response; myeloid-derived suppressor cells; tumour-infiltrating lymphocytes; tumour microenvironment; immunohistochemistry

Adaptive immune contexture at the tumour site and downmodulation of circulating myeloid-derived suppressor cells in the response of solitary fibrous tumour patients to anti-angiogenic therapy

M Tazzari[1,2], T Negri[2,3], F Rini[1,2], B Vergani[4], V Huber[1,2], A Villa[4], P Dagrada[2,3], C Colombo[2,5], M Fiore[2,5], A Gronchi[2,5], S Stacchiotti[2,6], P G Casali[2,6], S Pilotti[2,3], L Rivoltini[1,2] and C Castelli*[,1,2]

[1]Unit of Immunotherapy of Human Tumours, Department of Experimental Oncology and Molecular Medicine, Via G. Venezian 1, Milan 20133, Italy; [2]Fondazione IRCCS Istituto Nazionale dei Tumori, Via G. Venezian 1, Milan 20133, Italy; [3]Laboratory of Experimental Molecular Pathology, Department of Diagnostic Pathology and Laboratory, Via G. Venezian 1, Milan 20133, Italy; [4]Consorzio MIA (Microscopy and Image Analysis), University of Milano-Bicocca, Via G. Venezian 1, Milan 20133, Italy; [5]Department of Surgery, Via G. Venezian 1, Milan 20133, Italy and [6]Adult Sarcoma Medical Oncology Unit, Department of Cancer Medicine, Via G. Venezian 1, Milan 20133, Italy

Background: Host immunity is emerging as a key player in the prognosis and response to treatment of cancer patients. However, the impact of the immune system and its modulation by therapies are unknown in rare soft tissue sarcomas such as solitary fibrous tumours (SFTs), whose management in the advanced forms includes anti-angiogenic therapy. Here, we studied the *in situ* and systemic immune status of advanced SFT patients and the effects of sunitinib malate (SM) in association with the clinical efficacy.

Methods: Immune contexture of SFTs was assessed by immunohistochemistry in lesions from untreated or SM-treated patients. Frequency of circulating myeloid-derived suppressor cells (MDSCs), regulatory T cells (Tregs) and T-cell functions was assessed *ex vivo* in SFT patients prior and during anti-angiogenic therapy. Patients with long-term tumour control were included to correlate immune profiles and clinical responses.

Results: Anti-angiogenic naïve SFT lesions were heavily infiltrated by $CD163^+CD14^+CD68^-$ and $CD163^+CD14^-CD68^-$ myeloid cells but devoid of T cells. Conversely, post-SM tumours acquired a new subset of $CD68^+CD14^+$ myeloid cells and displayed traits of an on-going adaptive immunity, strongly enriched in activated $CD8^+$ and $CD4^+$ T cells. These changes at the tumour site paralleled the alleviation of systemic immunosuppression and the drop in the frequency of circulating monocytic MDSCs (mMDSCs) and granulocytic MDSCs (gMDSCs). Rebound in the number of mMDSCs, but not of gMDSCs occurred at disease progression, and a reduced percentages of mMDSCs, comparable to those found in healthy donors (HDs), endured only in the SM-responsive patients.

Conclusions: The immune contexture of SFT patients is heavily involved in anti-angiogenic therapy and it could be exploited to achieve more durable disease control through immune-based combination strategies.

*Correspondence: Dr C Castelli; E-mail: chiara.castelli@istitutotumori.mi.it

Revised 12 June 2014; accepted 3 July 2014; published online 7 August 2014

Solitary fibrous tumour (SFT) is a rare subtype of soft tissue sarcoma (STS) that can occur in several anatomical sites, most frequently in middle-aged patients. Whereas most SFTs have an indolent course and can be cured by surgery, 15–20% of SFTs progress with either local recurrence or distant metastases (Chan, 1997; Fletcher *et al*, 2013). In addition to the classical SFT (CSFT), two more aggressive clinical-pathological variants of SFTs are currently recognised: malignant (MSFT) and dedifferentiated (DSFT), the latter showing a high-grade sarcoma overgrowth (Mosquera and Fletcher, 2009; Collini *et al*, 2012). We and other groups have recently described the activity of sunitinib malate (SM) (Chow and Eckhardt, 2007), in unresectable, progressive M/DSFT patients (George *et al*, 2009; Stacchiotti *et al*, 2010, 2012). Apart from being an anti-angiogenic drug, SM possesses immunomodulatory functions (Ko *et al*, 2009; Ozao-Choy *et al*, 2009). The role of the immune system in controlling tumour growth has long been recognised and the immune contexture, defined by the frequency, type, functional polarisation and local distribution of immunocompetent cells at the tumour site, has been shown to impact tumour prognosis (Fridman *et al*, 2012; Galon *et al*, 2014). Moreover, 'avoiding immune destruction' has been recently listed as an emerging hallmark of cancer (Hanahan and Weinberg, 2011; Schreiber *et al*, 2011) and among the immune suppression mechanisms active in cancer patients, those mediated by Tregs and MDSCs strongly hinder the anti-tumour response in patients with cancer of different histology (Filipazzi *et al*, 2007; Diaz-Montero *et al*, 2009; Mougiakakos *et al*, 2010). Little is presently known about the nature and features of the immune response to SFT, and no accurate histological description of local immunity exists for this STS. Moreover, the impact of anti-cancer therapies on the immunological status of SFT patients remains unexplored. Herein, we showed that the immunological profiles of CSFT, MSFT and DSFT patients, at the tumour site and in circulating PBMCs, revealed an immunosuppressive status. Our data demonstrated that SM treatment relieves systemic immunosuppression in PBMCs of M/DSFT patients, and at the tumour site it favoured the setting of an immune contexture with typical adaptive immunity traits. Altogether, these findings pave the way for the design of therapies that combine immune-based approach with anti-angiogenic treatment in SFT patients to achieve a more durable control of this aggressive disease.

MATERIALS AND METHODS

Immunohistochemistry and confocal analysis. Serial sections of 5-μm thick formalin-fixed, paraffin-embedded (FFPE) SFT samples ($n = 19$) were cut and processed for immunohistochemistry (IHC) or immunofluorescence staining (see Supplementary materials and methods for details). The clinical and pathological characteristics of each tumour are summarised in Supplementary Table S1. All the tumour samples were analysed for the presence of the NAB2-STAT6 fusion as previously described (Mohajeri *et al*, 2013; Robinson *et al*, 2013) (see Supplementary materials and methods). The antibodies used for IHC and confocal analysis and their conditions of use are reported in Supplementary Table S2. Confocal microscopy was carried out using a Radiance 2100 microscope (Bio-Rad Laboratories, Hercules, CA, USA) equipped with a krypton/argon laser and a red laser diode. Evaluation of all IHC stains was performed by the Pathologist (SP) who scored the intensity of the staining using a scale from (−) no staining to (++++) very strong staining.

Blood sample collection and patient characteristics. This study was conducted in compliance with the Declaration of Helsinki and approved by the Ethical Committee of Fondazione IRCCS Istituto Nazionale dei Tumori, and all of the patients signed a written informed consent for the collection of blood samples. Blood samples were collected from SFT patients before and at different time points after initiating continuous treatment with anti-angiogenic therapy. Blood was also collected at the time of disease progression. Blood from age-matched healthy donors (HDs) was also obtained for control. PBMCs were isolated by Ficoll/Paque PLUS density gradient centrifugation within 2 h of the blood draw, as described elsewhere (Casati *et al*, 2006). To avoid assay-to-assay variability, purified PBMCs were cryopreserved in liquid nitrogen for batch acquisition of Tregs and MDSCs based on phenotype and frequency. Immunological monitoring of circulating Tregs and MDSCs was conducted in a total of 17 SFT patients. The clinical characteristics of patients are reported in Table 1. The mean duration of the anti-angiogenic treatment was 6 months (range, 1–20); patients underwent disease assessment at baseline and after ~1–2 months. Objective responses according to the Response Evaluation Criteria in Solid Tumors (RECIST) and tumour burden were determined by physician assessment of radiographs. Patients were treated until they experienced RECIST-defined disease progression or unacceptable toxicity.

SFT tumour dissociation and tumour-infiltrating lymphocytes analysis. Tumour-infiltrating lymphocytes (TILs) were obtained from tumour sample of patients who underwent surgery by enzymatic and mechanic digestion using the gentleMACS Dissociator (Miltenyi, Bergisch-Gladbach, Germany). Briefly, tumour specimens were minced under sterile conditions into small pieces and digested over 1 h at 37 °C following the gentle MACS Dissociator protocol (Miltenyi). The resulting cell suspension was filtered through a 70-μm mesh (BD Biosciences, San Jose, CA, USA), the red blood cells were lysed, and the cell suspension was washed with RPMI. Cells were stored in liquid nitrogen until use. For intracellular cytokine staining, patients' TILs were seeded into 96-well round-bottom plates at 1.5×10^5 cells per well in RPMI + 10% human serum and stimulated overnight with PMA and Ionomycin (50 and 500 ng ml^{-1}, respectively) plus GolgiStop (4 μl 6 ml^{-1}, BD Biosciences) at 37 °C. Tumour-infiltrating lymphocytes were stained for the cell-surface markers CD3, CD4 and CD8. The cells were then washed, fixed and permeabilised with Fix/Perm reagents (eBioscience, San Diego, CA, USA) following the manufacturer's protocol and then stained with a488-labelled anti-IFN-γ (BioLegend, San Diego, CA, USA), PE-labelled anti-Tbet (eBioscience) or PE-labelled anti-granzyme B (BD Biosciences). Dead cells were identified using the LIVE-DEAD Fixable Violet Dead Cell Stain Kit (Life Technologies, Carlsbad, CA, USA) according to the manufacturer's instructions and excluded from the analysis. The fluorescence intensity was measured using a Gallios (Beckman Coulter, Brea, CA, USA) flow cytometer and analysed using the Kaluza software (Tree Star Inc, Ashland, OR, USA).

Flow cytometry and intracellular cytokine staining. Treg and MDSC frequencies were determined by six-colour immunofluorescence staining of thawed PBMCs. The antibodies used are reported in Supplementary Table S3. Dead cells were identified using the LIVE-DEAD Fixable Violet Dead Cell Stain Kit (Life Technologies) and excluded from the analysis. For surface staining, cells were incubated with antibodies for 30 min at 4 °C after blocking non-specific antibody binding to the Fc receptors using FcR Blocking Reagent (Miltenyi). For Treg analysis, intracellular staining with APC-conjugated anti-Foxp3 (eBioscience) or the proper isotype control (rat IgG2a) was performed after fixation and permeabilisation of cells using an intracellular staining kit (eBioscience) according to the manufacturer's instructions. Intracellular staining was performed as follows. Lymphocytes activated overnight with anti-CD3/CD28 beads (DynaBeads CD3/CD28 T cell Expander, Invitrogen Dynal AS, Oslo, Norway) in the presence

Table1. Clinicopathologic characteristics of patients

Patient ID	Tumour site	Diagnosis	Drug treatment[a]	Response to SM: RECIST evaluation	PFS (months)
1a	Thigh	CSFT	–	–	–
2a	Abdomen	CSFT	–	–	–
3a	Abdomen	CSFT	–	–	–
4a	Pelvis	CSFT	–	–	–
5a	Thigh	CSFT	–	–	–
6a[b]	Pleura	MSFT	+	PR	12+
7a[c]	Pleura	MSFT	+	SD	6
8a[b]	Pleura	MSFT	+	SD	10
9a	Abdomen	MSFT	+	PD	1.5
10a[b,d]	Pelvis	MSFT	+	PR	20
11a	Pleura	MSFT	+	SD	5
12a[c,e]	Pleura	DSFT	+[f]	Not assessable[g]	–
13a[c]	Pleura	DSFT	+	PD	2
14a[c]	Meninges	DSFT	+	PD	1.5
15a	Pleura	DSFT	+	PD	2
16a	Peritoneum	DSFT	–	–	–
17a	Cerebellum	DSFT	–	–	–

Abbreviations: CSFT = classical solitary fibrous tumour; DSFT = dedifferentiated solitary fibrous tumour; MSFT = malignant solitary fibrous tumour; PD = progressive disease; PFS = progression-free survival; PR = partial response; RECIST = Response Evaluation Criteria in Solid Tumors; SD = stable disease; SM = sunitinib malate. Age (median; range): 56; 35–76; Gender (n and %): M 29%, F 71%; Male 5, Female 12.

[a]Patients received 37.5 mg per die of SM.

[b]PBMCs from the pre-treatment (PRE) period were not available for analysis.

[c]Patients had undergone a previous CT regimen. A washout period of at least 15 days was respected before entering SM treatment and beginning blood draws.

[d]For this patient, tumour removed after SM treatment was analysed by IHC and corresponded to Tumour ID #13 in Supplementary Table S1. TILs from Tumour ID #13 were analysed *ex vivo* for their functional activity.

[e]PBMCs at the time of progression were not available for analysis.

[f]This patient received 800 mg per die of pazopanib.

[g]Therapy interrupted due to toxicity.

of 1 μl ml^{-1} GolgiPlug (BD Biosciences) were stained for the cell-surface marker CD3. The cells were then washed, fixed and permeabilised with Cytofix/Cytoperm buffer (BD Biosciences) and stained with a488-labelled anti-IFN-γ (BioLegend), PE-labelled anti-IL-2 (BD Biosciences). Data acquisition was performed using a Gallios (Beckman Coulter) flow cytometer, and the Kaluza software was used for data analysis.

Intracellular protein kinase assay. Cryopreserved PBMCs were thawed, washed and rested 2 h at 37 °C in RPMI containing 1% HS. Then, cells were incubated either without stimulation or stimulated with GM-CSF 10 ng ml^{-1}, IL-4 100 ng ml^{-1}, VEGF 50 ng ml^{-1} (all from Peprotech, Rocky Hill, NJ, USA) and IFNα 10 000 U ml^{-1} (Sigma-Aldrich, St Louis, MO, USA). Immediately after stimulation cells were fixed with pre-warmed BD Cytofix Buffer (BD Biosciences) for 10 min at 37 °C. After incubation cells were washed with PBS 1% FCS and then stained with anti-CD14 APC alexa750 (Beckman Coulter) and HLA-DR FITC (BD Biosciences) for 30 min and permeabilised with Perm Buffer III solution (BD Biosciences). Cell were then stained for intracellular expression of anti-pSTAT1 (Y701) Alexa Fluor 647, -pSTAT3 (Y705) Alexa Fluor 647, -pSTAT6 (Y641) PE and -pSTAT5 (Y694) PE (all from BD Bioscences). Data were acquired on a Gallios (Beckman Coulter) flow cytometer and analysed using the Kaluza software.

Arginase activity assay. Plasma from HDs and SFT patients was tested for arginase activity by measuring the production of L-ornithine from L-arginine, as previously reported (Rodriguez *et al*, 2004). In brief, a mix of 25 μl of plasma and 25 μl of buffer (Tris-HCl 50 nM pH 7.5 plus 10 mM $MnCl_2$, Sigma-Aldrich) was heated at 55 °C for 20 min. Then, 150 μl carbonate buffer (100 mM; Sigma-Aldrich) and 50 μl L-arginine (100 mM; Sigma-Aldrich) were added and the mix incubated at 37 °C for 20 min. The hydrolysis of L-arginine was stopped with 750 μl of glacial acetic acid. In all, 250 μl of ninhydrin solution (2.5 g ninhydrin (Sigma-Aldrich); 40 ml H_3PO_4 6 M; 60 ml glacial acetic acid) was added followed by incubation at 95 °C for 1 h. The amount (nmol) of L-ornithine was determined measuring the absorbance at 570 nm.

Statistical analysis. The two-tailed unpaired Student's *t* test (with a 95% confidence interval (CI)) was used to compare groups, while the two-tailed paired Student's *t* test was used to analyse the effect of the treatments between different time points, as indicated in the figure legends. Statistical calculations were performed using the Prism5 software (GraphPad Software, La Jolla, CA, USA). *P*-values < 0.05 were considered as statistically significant. Error bars represent the standard error of the mean (s.e.m.).

RESULTS

Tumour-infiltrating immune cells in CSFT and M/DSFT. To gain insight into the immune contexture of SFTs, the presence and functional polarisation of tumour-infiltrating T cells and myeloid/macrophage cells were assessed by IHC analysis on a retrospective series of FFPE SFT specimens ($n = 11$) collected from patients who did not receive anti-angiogenic therapy before surgery. This series

of anti-angiogenic-naïve SFTs included three CSFTs, and five MSFTs and three DSFTs. Supplementary Table S1 reports the histopathological features of the studied tumours. The majority of the analysed samples were negative or very poorly infiltrated with $CD3^+$ T cells (Figure 1A). Only two cases (MSFT Tumour ID #8 and DSFT Tumour ID #9) displayed a remarkable positivity for CD3 staining (Figure 1A) that, however, was paralleled by a strong positivity for the Foxp3 nuclear marker, thus indicating enrichment in infiltrating Tregs (Figure 1A). In our samples, antibodies directed against the CD68 and CD163 markers did not stain tumour cells but did identify two different subgroups of tumour-associated macrophages (TAMs). All of the SFT cases displayed strong infiltration by $CD163^+$ cells intermingled with the tumour cells, and the frequency of this myeloid cell type was further enhanced in tumours with a worse prognosis, namely M/DSFT samples. Conversely, CD68 staining was completely negative or revealed only few/scattered positive cells (Figure 1A). Confocal analysis, performed to better clarify the nature of the myeloid cells present in the M/DSFT microenvironment, showed that the majority of the $CD163^+$ cells were positive for CD14, fitting with a pro-tumour, M2-TAM nature (Figure 1B, arrows) (Mantovani *et al*, 2002). Moreover, a subset of CD163 single-positive cells was also detected (Figure 1B, circle). According to the literature, these cells might represent a subset of myeloid progenitors or immature cells (de Vos van Steenwijk *et al*, 2013). Analysis of the granulocytic component was also performed and no evidence for a selective infiltration of this cell subset was evidenced. $CD66b^+$ cells were in fact only occasionally found inside the tumour, with some positivity detected only in perivascular areas (see Supplementary Figure S1). Collectively, the IHC and confocal analyses indicated poor T-cell infiltration and an immunological status skewed towards immune suppression in CSFT and in M/DSFT lesions.

		Marker expression			
Tumour ID	Diagnosis	CD3	Foxp3	CD163	CD68
1	CSFT	–	–	++	±
2	CSFT	±	–	++	–
3	CSFT	±	–	+	±
4	MSFT	–	/	+++	±
5	MSFT	–	/	++	±
6	MSFT	±	+	+	–
7	MSFT	–	/	+++	–
8	MSFT	++	+	++++	–
9	DSFT	+++	++	++++	±
10	DSFT	–	/	++	–
11	DSFT	–	/	+++	–

Summary of IHC results for anti-angiogenic naïve SFT lesions abbreviations: CSFT, classical solitary fibrous tumour; MSFT, malignant solitary fibrous tumour; DSFT, dedifferentiated solitary fibrous tumour; /, not done; –, no staining; ±, very weak; +, weak; ++ moderate; +++, stong; ++++, very strong.

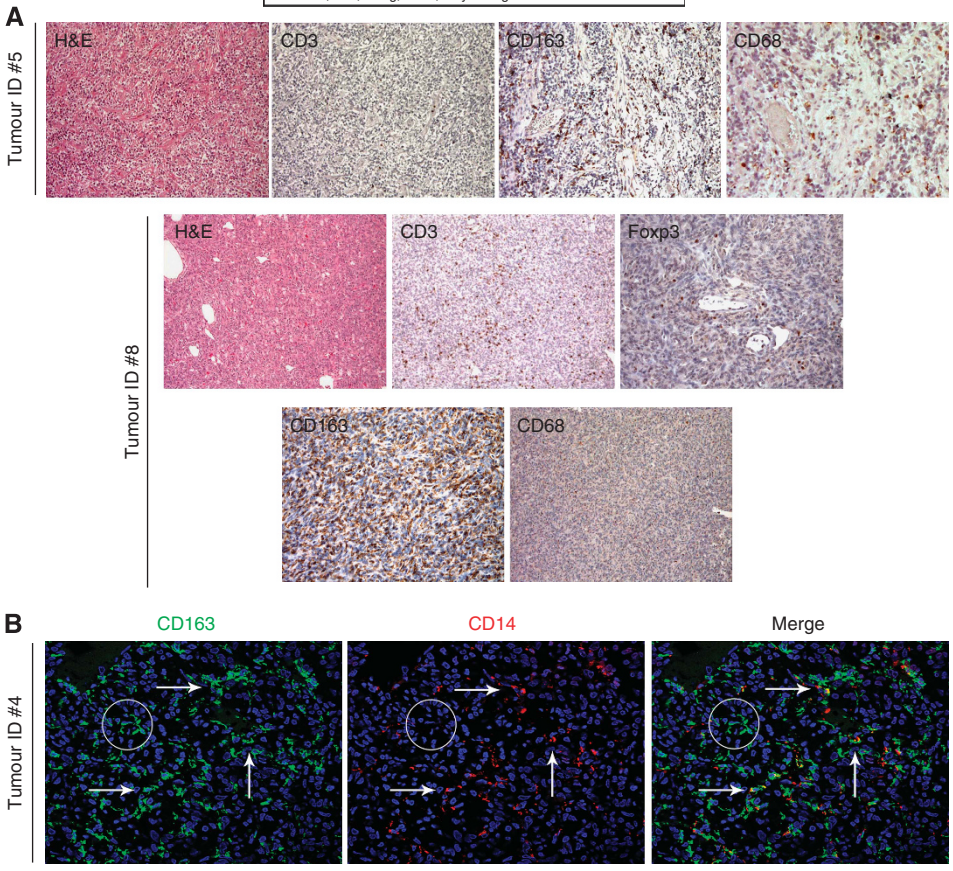

Figure 1. Analysis of tumour-infiltrating immune cells in M/DSFTs not treated with anti-angiogenic therapy. Representative IHC stainings of two targeted therapy-naïve MSFT lesions (Tumour IDs #5 and #8). (**A**) (H&E) Haematoxylin and eosin staining. Images show MSFT lesions (ID #5) with no or (ID #8) moderate CD3 infiltration. (ID #8) $CD3^+$ T cells showed positivity for the Foxp3 nuclear marker. (Tumour IDs #5 and #8) Presence of a very high density of CD163-positive macrophages diffusely dispersed among the cancer cells. (ID #5) Sparse or (ID #8) absence infiltration of $CD68^+$ macrophages. (**B**) (Tumour ID #4) Double-label immunofluorescence staining for CD163 (green) and CD14 (red) macrophage markers. The arrow indicates $CD163^+CD14^+$ cells. The circle identifies $CD163^+$ cells that do not express CD14.

Evidence of a distinct immune cell signature in M/DSFT lesions from SM-treated patients. Pro-angiogenic factors and abnormal tumour vasculature hamper the extravasation of immune cells into the tumour parenchyma and promote immune suppression (Dirkx *et al*, 2003). Conversely, anti-angiogenic treatments, while normalising blood vessels, enhance immune infiltration, as recently shown in different animal models (Shrimali *et al*, 2010; Jain, 2013). In M/DSFT patients, we recently described the activity of SM, and we reported that SM led to vascular normalisation at the tumour site (Stacchiotti *et al*, 2012). We thus explored the immune contexture in four M/DSFT lesions surgically removed from patients who received SM in neo-adjuvant setting.

All of these samples showed a high density of $CD3^+$ TILs (Figure 2A), which included both $CD4^+$ and $CD8^+$ T cells. The intratumoral lymphocytes were mainly HLA-DR positive, and a consistent fraction of them also stained positive for granzyme B (GZMB) and T cell-restricted intracellular antigen (TIA-1, a cytotoxic granule-associated protein expressed by cytotoxic T cells and involved in the induction of apoptosis in CTL-sensitive targets) (Figure 2A). Thus, the $CD3^+$ infiltrating cells were mainly activated T cells endowed with cytolytic potential. Moreover, their positivity for the nuclear transcription factor T-bet (immune cell-specific member of the T-box family of transcription factor coordinating type 1 immune responses) suggested enrichment in functional, Th-1-polarised T cells (Figure 2A). No $Foxp3^+$ cells were detected (Figure 2A), indicating the absence of regulatory, suppressive T cells at the tumour site in post-SM M/DSFT patients. Concerning the monocyte/macrophage compartment, in addition to the $CD163^+CD68^-$ myeloid population (Figure 3), post-SM M/DSFTs displayed a strong positivity for intratumoral $CD68^+$ myeloid cells (Figure 3A). On confocal analysis, these $CD68^+$ cells co-expressed CD14 and represented a newly acquired population of macrophages rarely found in untreated tumours (Figure 3Bb). Moreover, these $CD68^+$ macrophages displayed a typical round morphology, and double-immunofluorescence staining revealed co-expression of both the CD68 and HLA-DR markers (Figure 3Bc). These features are compatible with the M1 phenotype of activated macrophages. On IHC evaluation, all of the cases treated with SM showed signs of a pathologic response. Extensive areas of necrosis and tumour regression were observed in the proximity of the immune and inflammatory infiltration. Of note, around the area of tumour regression, $CD8^+$ and $CD4^+$ T cells were organised in clusters (Figure 2B). Altogether, the IHC results were consistent with an ongoing adaptive immunity in post-SM M/DSFTs. To strengthen this conclusion, *ex vivo* TILs were isolated from the excised naïve and post-SM MSFT (Patient ID #13) specimens and tested *in vitro* for their immunological properties. T cells from post-SM lesions were found to contain functionally active $CD4^+$ T cells producing IFN-γ *ex vivo* and $CD8^+$ GZMB-positive T cells, representing effector cytotoxic T lymphocytes (Figure 2C).

Standard treatment for M/DSFT patients includes different regimens of cytotoxic chemotherapy (CT) associated or not with radiotherapy (RT). To verify whether modulation of the immune contexture at the tumour site also occurred in patients responding to CT, IHC analysis was performed in four M/DSFT tumour lesions surgically removed from patients who received CT/RT in neo-adjuvant setting. Weak/moderate CD3 infiltration and only few, spared $CD68^+$ cells were detected in the two tumours post-CT (isofosfamide and/or epirubicin) plus RT (see Supplementary Figure S2; Tumour IDs #14 and #15). The absence of $CD68^+$ cells and very week $CD3^+$ T-cell infiltration characterised the post-epirubicin (monotherapy) tumour (see Supplementary Figure S2; Tumour ID #13). Of note, in the tumour sample from a patient treated with doxorubicin and dacarbazine, moderate $CD3^+$ infiltration, associated with a still week but more clusterised $CD68^+$ positive infiltrate was detected in the proximity of areas showing signs of necrosis and tumour regression likely suggesting a possible engagement of the immune response.

Accumulation of immunosuppressive cells in the peripheral blood of SFT patients. To evaluate the systemic immunological status of SFT patients, we explored the frequency of Tregs and MDSCs in the peripheral blood of a prospectively collected series of 17 SFT patients who included 5 patients with tumours classified as CSFTs, 6 as MSFTs and 6 as DSFTs (Table 1). PBMCs of HDs, matched for gender and age, were included as controls. Regulatory T cells, defined as $CD25^{hi}Foxp3^{hi}$ within a live-gated $CD3^+CD4^+$ cell population, were significantly expanded in M/DSFT patients compared with age-matched HDs ($n=11$) ($P=0.0008$, 1.04 ± 0.65 *vs* 2.57 ± 1.05); conversely, no statistically significant difference existed between HDs and CSFT patients (Figure 4A). The percentage of mMDSCs, first defined by our group as $CD11b^+CD14^+HLADR^{-/low}$ (Filipazzi *et al*, 2007; Hoechst *et al*, 2008; Walter *et al*, 2012), was significantly higher in subjects with both CSFTs and M/DSFTs than in HDs ($P=0.0398$, 6.19 ± 4.03; $P<0.0001$, 13.88 ± 6.56 *vs* 3.23 ± 1.31, respectively) (Figure 4B). No difference in the percentages of $Lin^-HLADR^-CD33^+$ MDSCs was detected between patients and HDs (data not shown). The overall frequency of $CD3^+CD4^+$ T cells and myeloid/monocyte $CD14^+CD11b^+$ cells did not differ significantly between patients and HDs (Figure 4C and D). Moreover, circulating $CD3^+$ T cells from CSFT and M/DSFT patients were functionally impaired. Figure 4E and F shows that the frequency of $CD3^+$ T cells that produced IFN-γ and IL-2 *ex vivo* was strongly reduced in patients' PBMCs compared with HDs. Altogether, these phenotypic and functional assays suggested a status of systemic immunosuppression in SFT patients.

Anti-angiogenic therapy modulates peripheral immunosuppressive cells in patients with M/DSFT. Our *in situ* analysis provided evidence that anti-angiogenic treatment reprogrammed the immune contexture of M/DSFTs and favoured the onset of an active T-cell immunity. To evaluate whether anti-angiogenic therapy also affected the systemic immunological status of patients with M/DSFT, we monitored the frequency of circulating Tregs and MDSCs in PBMCs from patients with M/DSFTs collected at different time points during SM ($n=6$ patients) or pazopanib ($n=1$ patient) therapy (Table 1). These anti-angiogenic drugs did not induce lymphopenia (data not shown). Interestingly, at the end of the second week of treatment (T15), the frequency of blood Tregs, evaluated within the $CD3^+CD4^+$ compartment (Figure 5A) or in the total number of live cells (see Supplementary Figure S3), was significantly reduced ($P=0.0020$, 2.63 ± 1.12 *vs* 1.41 ± 0.75; $P=0.0117$, 0.57 ± 0.37 *vs* 0.36 ± 0.26). This effect was long lasting, and it was maintained for the duration of the treatment ($P=0.0204$, 1.41 ± 0.75 *vs* 0.95 ± 0.48; $P=0.0403$, 0.36 ± 0.26 *vs* 0.22 ± 0.14). The frequency of circulating mMDSCs, within the monocytic compartment (Figure 5B) or in the total number of live cells (Supplementary Figure S3), was significantly reduced at T15 ($P=0.0040$, 11.93 ± 4.84 *vs* 6.27 ± 5.52; $P=0.0295$, 2.72 ± 2.18 *vs* 0.44 ± 0.31). An increase in mMDSC frequency occurred in all of the patients at the time of disease progression although patients were still under drug treatment ($P=0.0043$, 6.27 ± 5.52 *vs* 13.13 ± 5.86; $P=0.0030$ 0.44 ± 0.31 *vs* 1.8 ± 0.66) (Figure 5B). The MDSC population includes also gMDSCs. A consensus has been reached in considering human gMDSCs as $CD14^-CD66b^+$ and/or CD15+ activated neutrophils within total PBMCs or inside the Lin^-HLADR^- fraction, displaying low density (thus being co-purified with PBMCs during blood centrifugation) and releasing arginase I in the circulation (Zea *et al*, 2005; Rodriguez *et al*, 2009; Brandau *et al*, 2011). We thus assessed the frequency of this MDSC subtype in PBMC of M/DSFT by monitoring the $CD66b^+CD15^+$, or $CD66b^+Lin^-HLA\text{-}DR^-$ cells as done in others published studies (Zea *et al*, 2005;

Tumour ID	Diagnosis	T cell marker expression						
		CD3	CD4	CD8	Granzyme B	T-bet	TIA-1	Foxp3
6	MSFT	++	++	++	–	+	/	–
12	DSFT	++	++	++	++	+	+	–
13	MSFT	++++	+++	++	+	++	–	–
14	DSFT	++++	++	++	–	++	++	–

Summary of IHC results for post-SM M/DSFT lesions
Abbreviations: MSFT, malignant solitary fibrous tumour; DSFT, dedifferentiated solitary fibrous tumour; /, not done; –, no staining; ±, very weak; +, weak; ++ moderate; +++, strong; ++++, very strong.
The expression of TIA-1, T-bet and Granzyme B was evaluated inside the T-cell area.

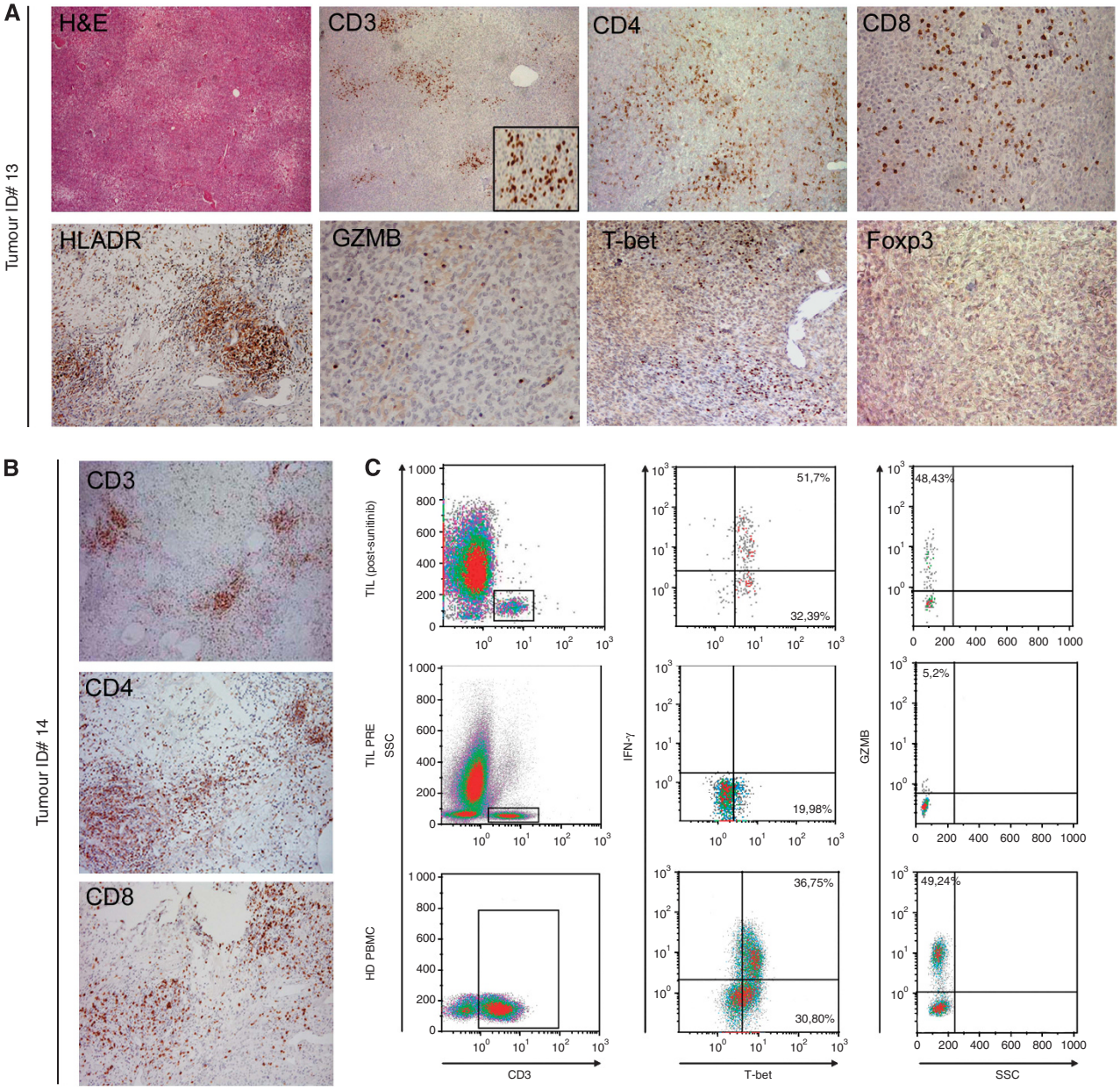

Figure 2. Analysis of infiltrating immune T cells in SM-treated M/DSFT lesions. (**A**) Representative IHC stainings of an SM-treated MSFT lesion (Tumour ID #13). (H&E) Haematoxylin and eosin stain. Staining for $CD3^+$ (low and high magnifications), $CD4^+$ and $CD8^+$ T cells is showed. Representative images of the expression of T cell-associated markers HLA-DR, granzyme B (GZMB), T-bet and Foxp3 are reported. (**B**) IHC analysis of an SM-treated DSFT lesion (Tumour ID #14) with evidence of tumour regression. In areas of tumour regression, T cells (CD3, CD4 and CD8) are organised in clusters. (**C**) Multi-parametric flow cytometry analysis of live lymphocytes from freshly dissociated naïve and SM-treated MSFT tumours (Tumour ID #13). Expression levels of T-bet, IFN-γ and GZMB were evaluated by intracellular flow cytometry in $CD3^+$ T cells. The gating strategy is reported.

Rodriguez *et al*, 2009; Brandau *et al*, 2011; Filipazzi *et al*, 2012) (Figure 5D). Moreover, for each M/DSFT patient, the arginase activity was quantified in the plasma and plotted along the absolute neutrophil count (Figure 5E). With respect to HDs, M/DSFT patients displayed an enhanced frequency of gMDSCs (Figure 5D) and an increased number of neutrophils in the blood (Figure 5E),

Tumour ID	Myeloid marker expression		
	Diagnosis	CD163	CD68
6	MSFT	+++	+++
12	DSFT	+++	+++
13	MSFT	++	++++
14	DSFT	+++	+++

Summary of IHC results for post-SM M/CDSFT lesions

Abbreviations: MSFT, malignant solitary fibrous tumour; DSFT, dedifferentiated solitary fibrous tumour; ++ moderate; +++, strong; ++++, very strong.

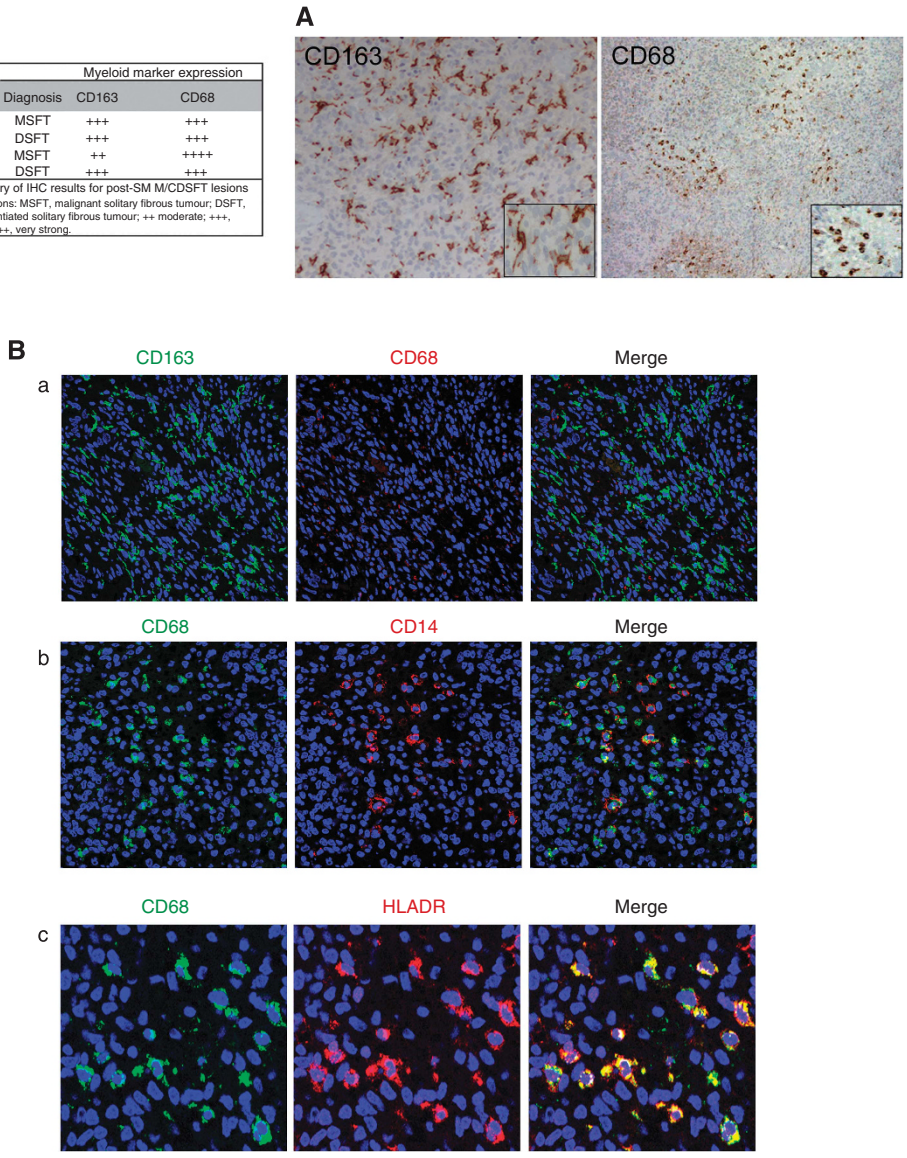

Figure 3. Analysis of infiltrating myeloid cells in SM-treated M/DSFT lesions. Stainings representative of an SM-treated MSFT lesion (Tumour ID #13). (**A**) IHC staining for the macrophage-associated markers CD163 and CD68 (low and high magnifications). (**B**) Double-label immunofluorescence staining and confocal analysis for (a) CD163 (green) and CD68 (red), (b) CD68 (green) and 14 (red), and (c) CD68 (green) and HLA-DR (red).

number that matched the higher plasma arginase activity. Frequency of gMDSCs, number of neutrophils and arginase activity were co-ordinately downmodulated by SM. However, similarly to Treg and at difference from mMDSCs, gMDSCs remained low all along the duration of SM treatment including at progressive disease (Figure 5D and E).

The functional assessment of the circulating $CD3^+$ T cells, which was based on their capacity to produce IFN-γ and IL-2 *ex vivo* (Figure 5F and G), revealed that immunosuppression, present in patient PBMCs before anti-angiogenic treatment (Figure 5F and G, PRE), was quickly relieved at T15. At progression, with the increase in mMDSCs, T cells displayed again an impaired function characterised by a limited IFN-γ and IL-2 production, similarly to what was found for the pre-treatment T cells.

Three patients displaying a long lasting response to SM treatment (Table 1, Pts #6a,8a,10a; SD or PR according RECIST evaluation after $\geqslant$10 months) consistently showed a low level of mMDSCs, with values comparable to HDs (Figure 6Aa) and no evidence of $CD3^+$ T-cell dysfunction in the peripheral blood could be detected in these SM-responsive patients (Figure 6Ab and c). Monocytic MDSCs from patients at time of disease progression were assessed for the activation of STAT-1, 3, 5 and 6 in response to the *ex vivo* cytokine stimulation. VEGF was unable to trigger STAT-3 phosphorylation in mMDSCs, likely as a result of the blocking activity exerted by SM. The other cytokines tested namely GM-CSF and IL-4, exerted their canonical activation pathways and induced STAT-5 and STAT-6 activation, respectively (data not shown). Conversely, these mMDSCs stimulated with IFNα, in addition to STAT-1 (data not shown), displayed a consistent phosphorylation of STAT-3. IFNα-dependent STAT-3 activation did not occurred in mMDSCs of HDs and SM-responsive patients (Figure 6B and C).

In summary, the analysis of the circulating immune cells in PBMCs from M/DSFT patients provided phenotypic and functional evidence of an immunosuppressive status that was quickly but temporary relieved by anti-angiogenic treatment. Suspension in the immunosuppression correlated with response to treatment.

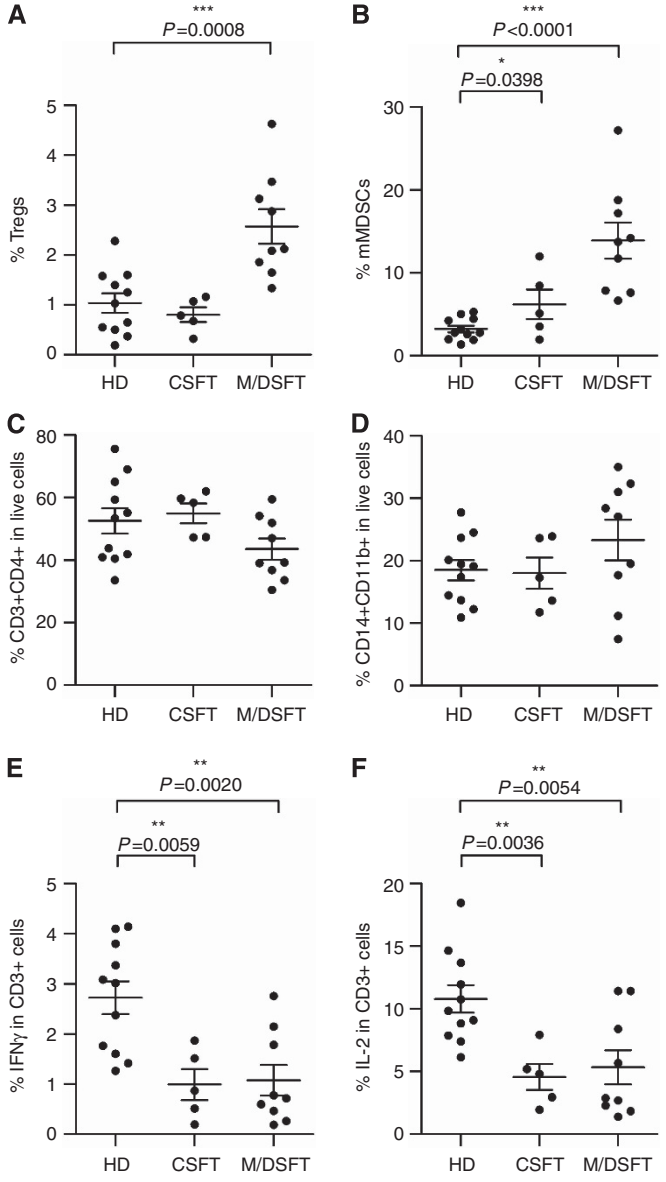

Figure 4. Accumulation of immunosuppressive cells in the peripheral blood of SFT patients. The frequencies of circulating Tregs and mMDSCs were monitored in the peripheral blood of CSFT ($n=5$) and M/DSFT ($n=9$) patients compared with healthy donors (HDs) ($n=11$). (**A**, **B**) Percentages of $CD25^{hi}Foxp3^{hi}$ cells (Tregs) and $CD11b^{+}CD14^{+}HLADR^{-/low}$ cells (mMDSCs) defined within $CD3^{+}CD4^{+}$ T cells and $CD14^{+}CD11b^{+}$ cells, respectively. (**C**, **D**) Analysis of peripheral $CD3^{+}CD4^{+}$ T lymphocytes and $CD11b^{+}CD14^{+}$ myeloid cells within live-gated PBMCs. (**E**) IFN-γ and (**F**) IL-2 intracellular staining was performed on PBMCs after anti-CD3/CD28 overnight stimulation. Analysis was performed on $CD3^{+}$-gated T cells. Each dot represents one patient. Statistical analysis: two-tailed unpaired Student's *t* test (95% confidence interval (CI)); only significant *P*-values are shown; bars indicate s.e.m.

DISCUSSION

To our knowledge, this is the first report that performed a detailed characterisation of the immunological status in the peripheral blood and at the tumour site of SFT patients and that considers the immune contexture of SFTs as a possible player in the response to therapy as well as in disease progression. Sunitinib malate exerts anti-tumour activity in M/DSFT (George *et al*, 2009; Stacchiotti *et al*, 2010, 2012) and patients achieving long-term tumour control have been reported (Domont *et al*, 2010; Levard *et al*, 2013). Besides the notion that immunity is emerging as a critical player in the response to treatment in cancer patients (Zitvogel *et al*, 2013), the rationale of assessing the role of the immune system in the efficacy of SM in SFTs stems from our previous observation that the levels of PDGFRβ and/or VEGFR2 activation, evaluated by IHC in tumour lesions, did not fully account for the therapeutic response to treatment (Stacchiotti *et al*, 2012).

The first interesting observation of our analysis was the presence of an immunosuppressed environment at the tumour site, characterised by a very dense infiltrate of myeloid cells and by the absence of granulocytic component. Myeloid cells, mostly CD68 negative, included $CD163^{+}CD14^{+}CD68^{-}$ TAMs, interdispersed among cancer cells and with an elongated, ramified morphology compatible with M2-type macrophages (Mantovani *et al*, 2002; Jensen *et al*, 2009; Caillou *et al*, 2011; Ino *et al*, 2013), together with $CD163^{+}CD14^{-}CD68^{-}$ cells likely representing immature myeloid-derived cells (Jensen *et al*, 2009; de Vos van Steenwijk *et al*, 2013). Conversely, $CD3^{+}$ lymphocytes were mainly absent, and when present, they were enriched in suppressive $Foxp3^{+}$ Tregs. An immunosuppressive status was also detectable in the peripheral blood of SFT patients. In fact, circulating T cells were consistently functionally impaired, and a significant accumulation of mMDSCs and gMDSCs was observed in all the patients analysed. Notably, the increased frequency of circulating mMDSCs (Figure 4B) and gMDSCs (data not shown) seemed to correlate with tumour grade and disease aggressiveness, being already detectable in CSFT patients and reaching the highest level in M/DSFT patients. The more compromised immune status of these patients with advanced SFTs was further confirmed by the additional accumulation of circulating Tregs, which instead showed frequency close to normal values in patients with CSFTs. Altogether, this scenario reveals a previously unappreciated tumour-mediated immunosuppression in SFT patients and particularly in patients with M/DSFTs. This observation opens the question whether this immunosuppressive signature can be reversed by anti-angiogenic treatments and whether re-activated tumour immunity could be part of the response to treatment. Noteworthy, no information about the immunological effect of SM, as detected *in situ* at the tumour site in human setting, are available to date. Our IHC analysis showed that, as opposed to SM-naïve tumours, SM-treated lesions were all characterised by a remarkable $CD3^{+}$ T-cell infiltration, with no $Foxp3^{+}$ Treg, but that included Th1 and cytotoxic-competent $CD4^{+}$ and $CD8^{+}$ T cells. Moreover, TILs purified from an SM-treated MSFT lesion released e*x vivo* Th1-related cytokines and cytotoxic GZMB, thus supporting the local engagement of a functionally active host immune response. Activated T cells at the tumour site correlated with the concomitant presence of a new subset of $CD68^{+}$ myeloid cells rarely found in untreated tumours. These $CD68^{+}$ macrophages displayed the round-shape morphology typical of the M1 polarisation (McWhorter *et al*, 2013), and expressed high level of HLA-DR. The pro-inflammatory and anti-tumour activity of $CD68^{+}$ macrophages infiltrating post-therapy SFTs is also supported by their organisation in clusters around the areas of tumour regression and in close proximity with activated T lymphocytes. Since macrophages display an elevated grade of plasticity in response to external stimuli (Mantovani *et al*, 2013), we may hypothesise that in SFTs, SM re-educated tumour-resident myeloid cells towards a more M1-related phenotype, or, alternatively, it recruited *ex novo* a new subset of monocytes/macrophages from peripheral blood.

Standard treatment for M/DSFT patients includes cytotoxic CT and/or RT. Evidence from the literature indicates that some CT regimens can be endowed with immunomodulatory activities

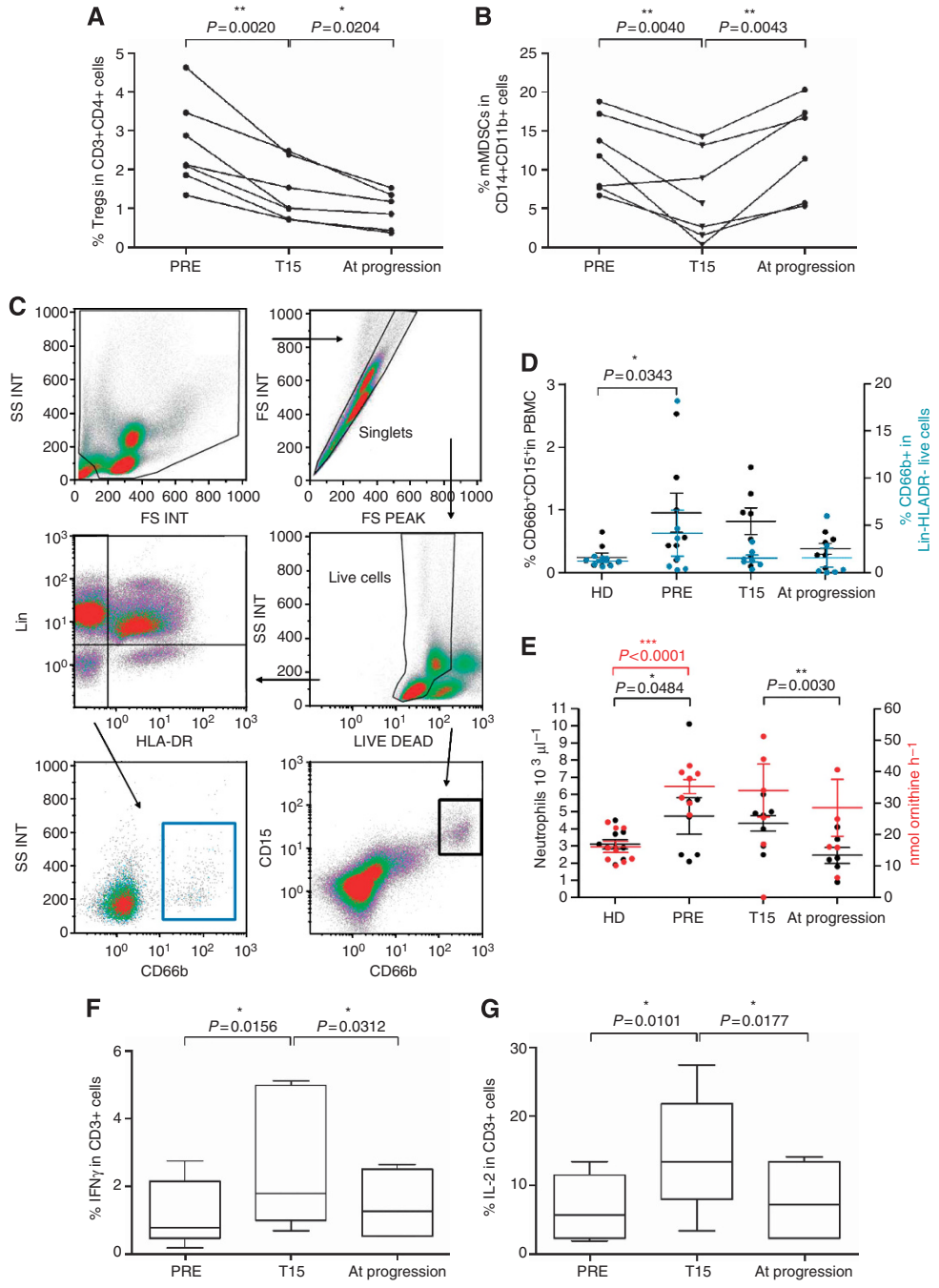

Figure 5. Anti-angiogenic therapy modulates immunosuppression in M/DSFT patients. (**A**, **B**, **D** and **E**) Anti-angiogenic therapy modulates the frequencies of immunoregulatory cells in M/DSFT patients. PBMCs of M/DSFT patients collected at three time points during anti-angiogenic treatment were analysed for the frequency of (**A**) $CD25^{hi}Foxp3^{hi}$ cells (Tregs) in $CD3^+CD4^+$ T cells and (**B**) $CD11b^+CD14^+HLADR^{-/low}$ cells (mMDSCs) in $CD14^+CD11b^+$ cells. (**C**) Gating strategy for gMDSC determination; (**D**) gMDSCs detected as $CD15^+CD66b^+$ in live-gated PBMCs (black) or as $CD66b^+$ cells within the $Lin^-HLA\text{-}DR^-$ fraction (light blue). (**E**) Absolute neutrophil count obtained by complete blood count (black dots), and arginase activity (red dots) evaluated as nmol ornithine per hour in 25 μl of patient's plasma. Each dot represents one patient; bars indicate s.e.m. PRE, PBMCs collected prior anti-angiogenic therapy; T15, PBMCs collected at day 15 during therapy; at progression, PBMCs collected at the time of disease progression. (**F**, **G**) Increased levels of circulating mMDSCs correlated with decreased T-cell functionality. PBMCs from M/DSFT patients ($n=7$) collected at different time points during anti-angiogenic treatment (PRE; T15; at progression) were assayed for (**F**) IFN-γ and (**G**) IL-2 after anti-CD3/CD28 overnight stimulation. Analysis was performed on $CD3^+$-gated T cells. The box plot depicts the median percentages of cytokine-positive $CD3^+$ T cells. Statistical analysis: two-tailed paired Student's *t* test (95% confidence interval (CI)); only significant *P*-values are shown; bars indicate s.e.m.

(Bracci *et al*, 2014). Analysis of the immune contexture was thus performed in M/DSFT tumours obtained from cytotoxic responsive patients. Only very mild modulation of the immune infiltration was observed and this occurred mainly in those cases receiving RT, thus confirming previously published data (Sharma *et al*, 2013). Of note, two of the analysed tumours, one that showed very few infiltration of T cells and the absence of myeloid cells (Tumour ID #13) and one treated with CT plus RT (Tumour ID #14),

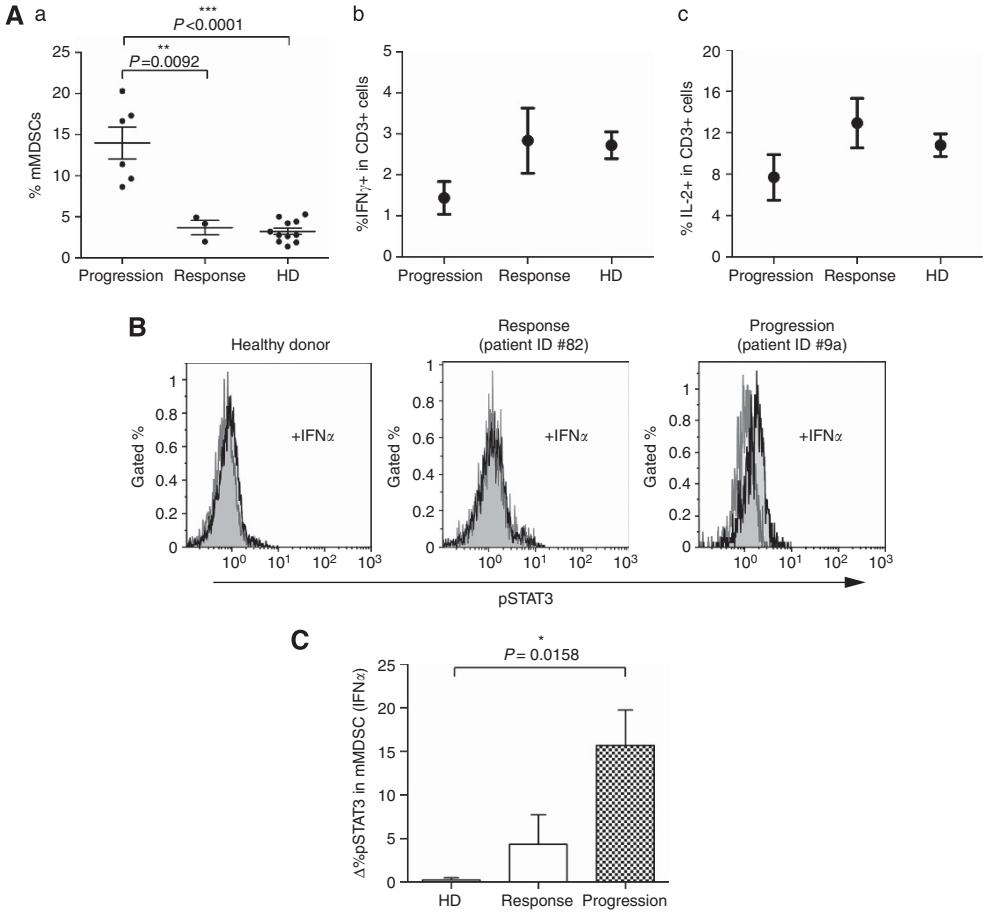

Figure 6. Modulation of mMDSCs in SM-treated M/DSFT patients. (**A**) Patients responding to SM treatment had normal levels of mMDSCs and did not display dysfunctional T cells. (a) Frequency of $CD11b^+CD14^+HLADR^{-/low}$ mMDSCs in PBMCs from M/DSFT patients treated with SM and displaying disease progression (Progression) or responsive to SM treatment (Response: 2 PR and 1 SD, duration of the response $\geqslant$10 months). The same PBMCs as in (a) were evaluated for the (b) frequency of $CD3^+$ T cells producing IFN-γ and (c) IL-2 after anti-CD3/CD28 overnight stimulation. (a) Each dot represents the data of a single patient. (b and c) Dot represents the mean value. (**B**) Representative histograms of pSTAT3 analyses in $CD11b^+CD14^+HLADR^{-/low}$ cells (mMDSCs) with (black) and without (grey) IFNα stimulation (10 000 U ml^{-1} for 15 min at 37 °C). (**C**) Columns represent the IFNα-induced STAT3 activation in $CD11b^+CD14^+HLADR^{-/low}$ cells of HDs ($n=4$), SM-responsive ($n=3$) and SM-progressive patients ($n=6$). Δ%pSTAT3 was calculated as: %pSTAT3 (IFNα) − %pSTAT3 (basal). Columns represent mean values; bars indicate s.e.m.

derived from patients subsequently treated and responding to SM and whose post-SM tumours were here analysed (Figure 2A and B). At difference from the autologous post-CT counterpart, post-SM tumours displayed a profound change in the tumour immune microenvironment with huge $CD3^+$ and $CD68^+$ infiltrating cells organised in cluster and intermingled with tumour cells and areas of tumour necrosis. A coordinated presence of $CD3^+$ and $CD68^+$ cell infiltration at lower density but with distribution similar to that observed in post-SM tumours was found in the sample treated with doxorubicin and dacarbazine, thus possibly testifying an involvement of the immune system in the response to this CT regimen. In summary, a modulation of both myeloid and lymphoid immune infiltrate occurred in all the four post-SM tumours, thus indicating a tight association between immune system and response to SM. This was not the case for the post-CT samples. However, the here analysed post-CT tumours were derived from patients who underwent heterogeneous CT treatments. Moreover, for the doxorubicin and dacarbazine regimen, a single case was available for testing. Consequently, definitive conclusions on the involvement of immune system into CT-induced response deserve further investigation. This is expressly true for the doxorubicin and dacarbazine CT in view of the fact that a retrospective study recently reported this CT regimen as effective in M/DSFT (Stacchiotti *et al*, 2013).

The ability of SM to interfere with myeloid cells, a property already suggested in other cancer patients (van Cruijsen *et al*, 2008; Ko *et al*, 2009), was further supported by our evidence that circulating mMDSCs and gMDSCs were significantly decreased in M/DSFT patients upon SM administration. The frequency of gMDSCs remained low and similar to the frequency found in HDs all along the duration of the treatment, including the time of progressive disease. Granulocytic MDSC behaviour thus overlapped that of Tregs and both these immunosuppressive cells might be considered as 'sensors/markers' of the pharmacologic activity of SM. The SM effect on mMDSCs might be more associated with disease control. In fact the recruitment of a new subset of $CD68^+$ myeloid cells expressing the CD14 marker occurred at the tumour site of patients responding to SM. Moreover, while SM-responsive patients ($n=3$, 1 SD and 2 PR according RECIST evaluation, mean duration time of response $\geqslant$10 months, Table 1) consistently displayed percentages of mMDSCs comparable to HDs, a rebound in the number of mMDSCs was observed at disease progression. Initial functional characterisation of mMDSCs analysed *ex vivo* from peripheral

blood of patients progressing during SM treatment revealed the capacity of these cells to promote STAT3 phophorylation upon IFNα stimulation. The IFNα-mediated STAT3 phophorylation did not occur in mMDSCs of SM-responding patients. The role of STAT3 in the development and effector functions of MDSCs is well documented in murine setting (Gabrilovich and Nagaraj, 2009) and recently suggested as crucial also for human mMDSCs (Poschke *et al*, 2010). However, the functional implication of this alternative STAT3 activation in mMDSC biology, and most importantly, the effects of anti-angiogenic therapy on such a signalling pathway deserve to be further explored. Nevertheless, these data together with the mMDSC boost at progression suggest that SM treatment might induce/select a qualitatively different mMDSC population, possibly representing an immune-mediated mechanism of acquired resistance. This 'immunological resistance to treatment' occurred only for the mMDSC compartment, as the SM-induced modulation of Treg and gMDSC frequency was detected in all the treated patients and it lasted for all the duration of the treatment.

In conclusion, our results shed light on a previously unappreciated phenomenon of immune dysfunction in this STS subtype and demonstrate that anti-angiogenic therapy opens a temporal window during which SFT patients regain normalisation in systemic myeloid differentiation status and T-cell functions thus, suggesting a contribution of the host immunity to the drug efficacy. Moreover, the rebound of circulating mMDSCs and impaired T-cell functions at tumour progression suggest that therapeutic strategies limiting residual myeloid suppressor activities (Nagaraj *et al*, 2010; Iclozan *et al*, 2013; Mok *et al*, 2013) and boosting tumour-specific immune responses represent a promising approach to improve the activity of anti-angiogenic treatment in SFT patients. Of note, the recent discovery that SFTs are marked by a tumour-specific chromosomal translocation (NAB2-STAT6) makes this tumour type an attractive target for active immunotherapy (Mohajeri *et al*, 2013; Robinson *et al*, 2013). In fact, the chimeric protein encoded by the recombinant *NAB2-STAT6* gene is a potential reservoir of unique tumour-specific antigens that are now considered as crucial in the design of an efficient personalised immunotherapy (Nadler and Schultze, 2002; Robbins *et al*, 2013; Tran *et al*, 2014).

ACKNOWLEDGEMENTS

We thank Dr Paola Frati and Mrs Felicetta Giardino (Unit of Immunotherapy of Human Tumors, Fondazione IRCCS Istituto Nazionale dei Tumori, Milan, Italy) for their precious clinical help. We are grateful to Dr Valeria Beretta (Unit of Immunotherapy of Human Tumors, Fondazione IRCCS Istituto Nazionale dei Tumori, Milan, Italy) for expert technical help. We are grateful to Dr Maria Grazia Daidone for coordinating the activities of the Tissue Bank internal to our institution. This study was supported by AIRC (Associazione Italiana Ricerca sul Cancro) (IG grants: CC (10615), SP (10300), and LR (10727); MFAG grant: TN (11817)). MT is supported by a fellowship from FIRC (Fondazione Italiana Ricerca sul Cancro).

CONFLICT OF INTEREST

SS received Pfizer coverage for medical meetings and research funding. CPG received Pfizer advisory honoraria and research funding. The remaining authors declare no conflict of interest.

AUTHOR CONTRIBUTIONS

MT, TN, BV, VH, SS, LR, SP and C Castelli made intellectual contributions to the conception and/or design of the study. MT and FR conducted the experiments. BV and AV designed and performed the immunohistochemical and confocal analysis. C Colombo, MF and AG performed selection and clinical evaluation of patients. MT, TN, BV, AV, SS, LR, SP and C Castelli were involved in the interpretation of data. All of the authors were involved in drafting and/or critical revisions of the manuscript and approved the final submitted version.

REFERENCES

Bracci L, Schiavoni G, Sistigu A, Belardelli F (2014) Immune-based mechanisms of cytotoxic chemotherapy: implications for the design of novel and rationale-based combined treatments against cancer. *Cell Death Differ* **21**: 15–25.

Brandau S, Trellakis S, Bruderek K, Schmaltz D, Steller G, Elian M, Suttmann H, Schenck M, Welling J, Zabel P, Lang S (2011) Myeloid-derived suppressor cells in the peripheral blood of cancer patients contain a subset of immature neutrophils with impaired migratory properties. *J Leukoc Biol* **89**: 311–317.

Caillou B, Talbot M, Weyemi U, Pioche-Durieu C, Al Ghuzlan A, Bidart JM, Chouaib S, Schlumberger M, Dupuy C (2011) Tumor-associated macrophages (TAMs) form an interconnected cellular supportive network in anaplastic thyroid carcinoma. *PLoS One* **6**: e22567.

Casati C, Camisaschi C, Rini F, Arienti F, Rivoltini L, Triebel F, Parmiani G, Castelli C (2006) Soluble human LAG-3 molecule amplifies the in vitro generation of type 1 tumor-specific immunity. *Cancer Res* **66**: 4450–4460.

Chan JK (1997) Solitary fibrous tumour-everywhere, and a diagnosis in vogue. *Histopathology* **31**: 568–576.

Chow LQ, Eckhardt SG (2007) Sunitinib: from rational design to clinical efficacy. *J Clin Oncol* **25**: 884–896.

Collini P, Negri T, Barisella M, Palassini E, Tarantino E, Pastorino U, Gronchi A, Stacchiotti S, Pilotti S (2012) High-grade sarcomatous overgrowth in solitary fibrous tumors: a clinicopathologic study of 10 cases. *Am J Surg Pathol* **36**: 1202–1215.

de Vos van Steenwijk PJ, Ramwadhdoebe TH, Goedemans R, Doorduijn EM, van Ham JJ, Gorter A, van Hall T, Kuijjer ML, van Poelgeest MI, van der Burg SH, Jordanova ES (2013) Tumor-infiltrating CD14-positive myeloid cells and CD8-positive T-cells prolong survival in patients with cervical carcinoma. *Int J Cancer* **133**: 2884–2894.

Diaz-Montero CM, Salem ML, Nishimura MI, Garrett-Mayer E, Cole DJ, Montero AJ (2009) Increased circulating myeloid-derived suppressor cells correlate with clinical cancer stage, metastatic tumor burden, and doxorubicin-cyclophosphamide chemotherapy. *Cancer Immunol Immunother* **58**: 49–59.

Dirkx AE, Oude Egbrink MG, Kuijpers MJ, van der Niet ST, Heijnen VV, Bouma-ter Steege JC, Wagstaff J, Griffioen AW (2003) Tumor angiogenesis modulates leukocyte-vessel wall interactions in vivo by reducing endothelial adhesion molecule expression. *Cancer Res* **63**: 2322–2329.

Domont J, Massard C, Lassau N, Armand JP, Le Cesne A, Soria JC (2010) Hemangiopericytoma and antiangiogenic therapy: clinical benefit of antiangiogenic therapy (sorafenib and sunitinib) in relapsed malignant haemangioperyctoma /solitary fibrous tumour. *Invest New Drugs* **28**: 199–202.

Filipazzi P, Valenti R, Huber V, Pilla L, Canese P, Iero M, Castelli C, Mariani L, Parmiani G, Rivoltini L (2007) Identification of a new subset of myeloid suppressor cells in peripheral blood of melanoma patients with modulation by a granulocyte-macrophage colony-stimulation factor-based antitumor vaccine. *J Clin Oncol* **25**: 2546–2553.

Filipazzi P, Huber V, Rivoltini L (2012) Phenotype, function and clinical implications of myeloid-derived suppressor cells in cancer patients. *Cancer Immunol Immunother* **61**: 255–263.

Fletcher CDM, Bridge JA, Hogendoorn PCW, Mertens F (2013) *World Health Organization Classification of Tumours of Soft Tissue and Bone,* 4th edn. IARC Press: Lyon.

Fridman WH, Pages F, Sautes-Fridman C, Galon J (2012) The immune contexture in human tumours: impact on clinical outcome. *Nat Rev Cancer* **12**: 298–306.

Gabrilovich DI, Nagaraj S (2009) Myeloid-derived suppressor cells as regulators of the immune system. *Nat Rev Immunol* **9**: 162–174.

Galon J, Mlecnik B, Bindea G, Angell HK, Berger A, Lagorce C, Lugli A, Zlobec I, Hartmann A, Bifulco C, Nagtegaal ID, Palmqvist R, Masucci GV, Botti G, Tatangelo F, Delrio P, Maio M, Laghi L, Grizzi F, Asslaber M, D'Arrigo C, Vidal-Vanaclocha F, Zavadova E, Chouchane L, Ohashi PS, Hafezi-Bakhtiari S, Wouters BG, Roehrl M, Nguyen L, Kawakami Y, Hazama S, Okuno K, Ogino S, Gibbs P, Waring P, Sato N, Torigoe T, Itoh K, Patel PS, Shukla SN, Wang Y, Kopetz S, Sinicrope FA, Scripcariu V, Ascierto PA, Marincola FM, Fox BA, Pages F (2014) Towards the introduction of the 'Immunoscore' in the classification of malignant tumours. *J Pathol* **232**: 199–209.

George S, Merriam P, Maki RG, Van den Abbeele AD, Yap JT, Akhurst T, Harmon DC, Bhuchar G, O'Mara MM, D'Adamo DR, Morgan J, Schwartz GK, Wagner AJ, Butrynski JE, Demetri GD, Keohan ML (2009) Multicenter phase II trial of sunitinib in the treatment of nongastrointestinal stromal tumor sarcomas. *J Clin Oncol* **27**: 3154–3160.

Hanahan D, Weinberg RA (2011) Hallmarks of cancer: the next generation. *Cell* **144**: 646–674.

Hoechst B, Ormandy LA, Ballmaier M, Lehner F, Kruger C, Manns MP, Greten TF, Korangy F (2008) A new population of myeloid-derived suppressor cells in hepatocellular carcinoma patients induces CD4(+)CD25(+)Foxp3(+) T cells. *Gastroenterology* **135**: 234–243.

Iclozan C, Antonia S, Chiappori A, Chen DT, Gabrilovich D (2013) Therapeutic regulation of myeloid-derived suppressor cells and immune response to cancer vaccine in patients with extensive stage small cell lung cancer. *Cancer Immunol Immunother* **62**: 909–918.

Ino Y, Yamazaki-Itoh R, Shimada K, Iwasaki M, Kosuge T, Kanai Y, Hiraoka N (2013) Immune cell infiltration as an indicator of the immune microenvironment of pancreatic cancer. *Br J Cancer* **108**: 914–923.

Jain RK (2013) Normalizing tumor microenvironment to treat cancer: bench to bedside to biomarkers. *J Clin Oncol* **31**: 2205–2218.

Jensen TO, Schmidt H, Moller HJ, Hoyer M, Maniecki MB, Sjoegren P, Christensen IJ, Steiniche T (2009) Macrophage markers in serum and tumor have prognostic impact in American Joint Committee on Cancer stage I/II melanoma. *J Clin Oncol* **27**: 3330–3337.

Ko JS, Zea AH, Rini BI, Ireland JL, Elson P, Cohen P, Golshayan A, Rayman PA, Wood L, Garcia J, Dreicer R, Bukowski R, Finke JH (2009) Sunitinib mediates reversal of myeloid-derived suppressor cell accumulation in renal cell carcinoma patients. *Clin Cancer Res* **15**: 2148–2157.

Levard A, Derbel O, Meeus P, Ranchere D, Ray-Coquard I, Blay JY, Cassier PA (2013) Outcome of patients with advanced solitary fibrous tumors: the Centre Leon Berard experience. *BMC Cancer* **13**: 109–2407-13-109.

Mantovani A, Biswas SK, Galdiero MR, Sica A, Locati M (2013) Macrophage plasticity and polarization in tissue repair and remodelling. *J Pathol* **229**: 176–185.

Mantovani A, Sozzani S, Locati M, Allavena P, Sica A (2002) Macrophage polarization: tumor-associated macrophages as a paradigm for polarized M2 mononuclear phagocytes. *Trends Immunol* **23**: 549–555.

McWhorter FY, Wang T, Nguyen P, Chung T, Liu WF (2013) Modulation of macrophage phenotype by cell shape. *Proc Natl Acad Sci USA* **110**: 17253–17258.

Mohajeri A, Tayebwa J, Collin A, Nilsson J, Magnusson L, von Steyern FV, Brosjo O, Domanski HA, Larsson O, Sciot R, Debiec-Rychter M, Hornick JL, Mandahl N, Nord KH, Mertens F (2013) Comprehensive genetic analysis identifies a pathognomonic NAB2/STAT6 fusion gene, nonrandom secondary genomic imbalances, and a characteristic gene expression profile in solitary fibrous tumor. *Genes Chromosomes Cancer* **52**: 873–886.

Mok S, Koya RC, Tsui C, Xu J, Robert L, Wu L, Graeber T, West BL, Bollag G, Ribas A (2013) Inhibition of CSF1 receptor improves the anti-tumor efficacy of adoptive cell transfer immunotherapy. *Cancer Res* **74**(1): 153–161.

Mosquera JM, Fletcher CD (2009) Expanding the spectrum of malignant progression in solitary fibrous tumors: a study of 8 cases with a discrete anaplastic component–is this dedifferentiated SFT? *Am J Surg Pathol* **33**: 1314–1321.

Mougiakakos D, Choudhury A, Lladser A, Kiessling R, Johansson CC (2010) Regulatory T cells in cancer. *Adv Cancer Res* **107**: 57–117.

Nadler LM, Schultze JL (2002) From genomics to cancer vaccines: patient-tailored or universal vaccines? *Curr Opin Mol Ther* **4**: 572–576.

Nagaraj S, Youn JI, Weber H, Iclozan C, Lu L, Cotter MJ, Meyer C, Becerra CR, Fishman M, Antonia S, Sporn MB, Liby KT, Rawal B, Lee JH, Gabrilovich DI (2010) Anti-inflammatory triterpenoid blocks immune suppressive function of MDSCs and improves immune response in cancer. *Clin Cancer Res* **16**: 1812–1823.

Ozao-Choy J, Ma G, Kao J, Wang GX, Meseck M, Sung M, Schwartz M, Divino CM, Pan PY, Chen SH (2009) The novel role of tyrosine kinase inhibitor in the reversal of immune suppression and modulation of tumor microenvironment for immune-based cancer therapies. *Cancer Res* **69**: 2514–2522.

Poschke I, Mougiakakos D, Hansson J, Masucci GV, Kiessling R (2010) Immature immunosuppressive CD14+HLA-DR-/low cells in melanoma patients are Stat3hi and overexpress CD80, CD83, and DC-sign. *Cancer Res* **70**: 4335–4345.

Robbins PF, Lu YC, El-Gamil M, Li YF, Gross C, Gartner J, Lin JC, Teer JK, Cliften P, Tycksen E, Samuels Y, Rosenberg SA (2013) Mining exomic sequencing data to identify mutated antigens recognized by adoptively transferred tumor-reactive T cells. *Nat Med* **19**: 747–752.

Robinson DR, Wu YM, Kalyana-Sundaram S, Cao X, Lonigro RJ, Sung YS, Chen CL, Zhang L, Wang R, Su F, Iyer MK, Roychowdhury S, Siddiqui J, Pienta KJ, Kunju LP, Talpaz M, Mosquera JM, Singer S, Schuetze SM, Antonescu CR, Chinnaiyan AM (2013) Identification of recurrent NAB2-STAT6 gene fusions in solitary fibrous tumor by integrative sequencing. *Nat Genet* **45**: 180–185.

Rodriguez PC, Quiceno DG, Zabaleta J, Ortiz B, Zea AH, Piazuelo MB, Delgado A, Correa P, Brayer J, Sotomayor EM, Antonia S, Ochoa JB, Ochoa AC (2004) Arginase I production in the tumor microenvironment by mature myeloid cells inhibits T-cell receptor expression and antigen-specific T-cell responses. *Cancer Res* **64**: 5839–5849.

Rodriguez PC, Ernstoff MS, Hernandez C, Atkins M, Zabaleta J, Sierra R, Ochoa AC (2009) Arginase I-producing myeloid-derived suppressor cells in renal cell carcinoma are a subpopulation of activated granulocytes. *Cancer Res* **69**: 1553–1560.

Schmielau J, Finn OJ (2001) Activated granulocytes and granulocyte-derived hydrogen peroxide are the underlying mechanism of suppression of t-cell function in advanced cancer patients. *Cancer Res* **61**: 4756–4760.

Sharma A, Bode B, Studer G, Moch H, Okoniewski M, Knuth A, von Boehmer L, van den Broek M (2013) Radiotherapy of human sarcoma promotes an intratumoral immune effector signature. *Clin Cancer Res* **19**: 4843–4853.

Schreiber RD, Old LJ, Smyth MJ (2011) Cancer immunoediting: integrating immunity's roles in cancer suppression and promotion. *Science* **331**: 1565–1570.

Shrimali RK, Yu Z, Theoret MR, Chinnasamy D, Restifo NP, Rosenberg SA (2010) Antiangiogenic agents can increase lymphocyte infiltration into tumor and enhance the effectiveness of adoptive immunotherapy of cancer. *Cancer Res* **70**: 6171–6180.

Stacchiotti S, Negri T, Libertini M, Palassini E, Marrari A, De Troia B, Gronchi A, Dei Tos AP, Morosi C, Messina A, Pilotti S, Casali PG (2012) Sunitinib malate in solitary fibrous tumor (SFT). *Ann Oncol* **23**: 3171–3179.

Stacchiotti S, Negri T, Palassini E, Conca E, Gronchi A, Morosi C, Messina A, Pastorino U, Pierotti MA, Casali PG, Pilotti S (2010) Sunitinib malate and figitumumab in solitary fibrous tumor: patterns and molecular bases of tumor response. *Mol Cancer Ther* **9**: 1286–1297.

Stacchiotti S, Tortoreto M, Bozzi F, Tamborini E, Morosi C, Messina A, Libertini M, Palassini E, Cominetti D, Negri T, Gronchi A, Pilotti S, Zaffaroni N, Casali PG (2013) Dacarbazine in solitary fibrous tumor: a case series analysis and preclinical evidence vis-a-vis temozolomide and antiangiogenics. *Clin Cancer Res* **19**: 5192–5201.

Tran E, Turcotte S, Gros A, Robbins PF, Lu YC, Dudley ME, Wunderlich JR, Somerville RP, Hogan K, Hinrichs CS, Parkhurst MR, Yang JC, Rosenberg SA (2014) Cancer immunotherapy based on mutation-specific CD4+ T cells in a patient with epithelial cancer. *Science* **344**: 641–645.

van Cruijsen H, van der Veldt AA, Vroling L, Oosterhoff D, Broxterman HJ, Scheper RJ, Giaccone G, Haanen JB, van den Eertwegh AJ, Boven E, Hoekman K, de Gruijl TD (2008) Sunitinib-induced myeloid lineage redistribution in renal cell cancer patients: CD1c+ dendritic cell frequency predicts progression-free survival. *Clin Cancer Res* **14**: 5884–5892.

Walter S, Weinschenk T, Stenzl A, Zdrojowy R, Pluzanska A, Szczylik C, Staehler M, Brugger W, Dietrich PY, Mendrzyk R, Hilf N, Schoor O, Fritsche J, Mahr A, Maurer D, Vass V, Trautwein C, Lewandrowski P, Flohr C, Pohla H, Stanczak JJ, Bronte V, Mandruzzato S, Biedermann T, Pawelec G, Derhovanessian E, Yamagishi H, Miki T, Hongo F, Takaha N, Hirakawa K, Tanaka H, Stevanovic S, Frisch J, Mayer-Mokler A, Kirner A,

Rammensee HG, Reinhardt C, Singh-Jasuja H (2012) Multipeptide immune response to cancer vaccine IMA901 after single-dose cyclophosphamide associates with longer patient survival. *Nat Med* **18**: 1254–1261.

Zea AH, Rodriguez PC, Atkins MB, Hernandez C, Signoretti S, Zabaleta J, McDermott D, Quiceno D, Youmans A, O'Neill A, Mier J, Ochoa AC (2005) Arginase-producing myeloid suppressor cells in renal cell carcinoma patients: a mechanism of tumor evasion. *Cancer Res* **65**: 3044–3048.

Zitvogel L, Galluzzi L, Smyth MJ, Kroemer G (2013) Mechanism of action of conventional and targeted anticancer therapies: reinstating immunosurveillance. *Immunity* **39**: 74–88.

Supplementary Information accompanies this paper on British Journal of Cancer website (http://www.nature.com/bjc)